

# Functionally Graded Thermal Barrier Composite Coatings Formed by Gas Tunnel Type Plasma Spraying

Akira KOBAYASHI

JWRI, Osaka University  
11-1 Mihogaoka,  
Ibaraki, Osaka 567-0047, Japan  
Email: [kobayasi@jwri.osaka-u.ac.jp](mailto:kobayasi@jwri.osaka-u.ac.jp)

## Abstract

*Zirconia ( $ZrO_2$ ) coating has superior property as thermal barrier coatings (TBC), and has been used in high-temperature turbine blade applications etc. This comes from the reason that  $ZrO_2$  has high temperature resistance, low thermal conductivity, and thermal shock resistance, etc. The porosity in the  $ZrO_2$  coating by plasma spraying has also an advantage for thermal insulation. While, it causes the problem that there is substrate's corrosion at high temperature because of high porosity in the coating. Therefore in order to use  $ZrO_2$  coating as TBC at high temperature operation, such as engine parts, the much denser coating has been demanded to prevent such corrosion. One of the key of the solution will be the graded functionality of the TBC.*

*Zirconia-alumina ( $ZrO_2$ - $Al_2O_3$ ) composite coating formed by the gas tunnel type plasma spraying at short spraying distance, has a high hardness layer at the surface side of the coating. The Vickers hardness ( $H_v=1300$ ) of the  $ZrO_2$  composite coating is much higher than zirconia ( $ZrO_2$ ) coating, and the graded functionality becomes large. In this paper, the graded functionality of such high hardness  $ZrO_2$  and its composite coating in the case of different spraying condition was investigated. And the enhancement of the graded functionality of such composite coatings was discussed. For these composite coatings, the Vickers hardness of high hardness layer near the coating surface became higher as the increase in the traverse number of plasma spraying. In the case of large traverse number, the hardness distribution was much smoother, and that the graded functionality was improved much better. The microstructure of this composite coating has a distribution of embedded thin  $ZrO_2$  splats in a  $Al_2O_3$  matrix, parallel alignment of the splats relative to the substrate surface, and so on.*

**Keywords:** Graded functionality, Zirconia-alumina composite coating, High hardness, Gas tunnel type plasma spraying, Traverse number, Microstructure, Vickers hardness, Thermal barrier coating

## 1. Introduction

Ceramic coatings have generally excellent characteristics such as corrosion resistance, thermal resistance wear resistance, and so on. Particularly, Zirconia ( $ZrO_2$ ) coating has superior property as thermal barrier coatings (TBC), and has been used in high-temperature turbine blade applications etc. This comes from the reason that  $ZrO_2$  has high temperature resistance, low thermal conductivity, and thermal shock resistance, etc. [1]. The porosity in the  $ZrO_2$  coating by plasma spraying has also an advantage for thermal insulation. While, it causes the problem that there is substrate's corrosion at high temperature because of high porosity in the coating. Therefore in order to use  $ZrO_2$  coating as TBC at high temperature operation, such as engine parts, the much denser coating has been demanded to prevent such corrosion. One of the key of the solution will be the graded functionality of the TBC.

Recently, the high functionally graded coatings (FGC) of ceramics are applied to many fields such as electronics and so on. However, the development of FGC for the corrosion protection at high temperature using plasma spray techniques is still in an embryonic stage and will require significant R&D efforts [2].

In these circumstances, the study on the ceramic sprayed coatings using the gas tunnel type plasma spraying newly developed had been started by the authors [3,4]. The fundamental properties of ceramic coatings formed by the gas tunnel type plasma spraying have been investigated in detail in the previous studies [5,6,7]. In this case, the Vickers hardness of this sprayed coating became 20-30 % higher than that of conventional plasma spraying. For example, In the case of alumina ( $Al_2O_3$ ) coatings, high hardness of  $H_v=1500$  was obtained at spraying distance  $L=30mm$  when the power input  $P=30$  kW [8,9].

In  $ZrO_2$  coating by means of the gas tunnel type plasma spraying, the Vickers hardness of the cross section was also increased with decreasing spraying distance  $L$ , and a higher Vickers hardness  $H_v$  could be obtained at a shorter spraying distance. For example, Vickers hardness of  $ZrO_2$  coating was  $H_v=1050$  at  $L=30$  mm, when  $P=20$  kW. And at  $L=30$  mm when  $P=33$  kW, the Vickers hardness of  $ZrO_2$  coating was about  $H_v=1200$  [10]. Thus,  $ZrO_2$  coating formed by the gas tunnel type plasma spraying at a short spraying distance has a high hardness layer at the surface side of the coating, which shows the graded functionality of hardness[11,12,13].

In this paper, the graded functionality of such high hardness  $ZrO_2$  and its composite coating (TBC) in the case of different spraying condition was investigated. The Vickers hardness of high hardness layer near the coating surface was investigated briefly, by changing the traverse number of plasma spraying. The influences on the microstructure of the coating and the coating density were also discussed.

## 2. Experimental Procedure

The gas tunnel type plasma spraying apparatus used in this study is shown in **Fig.1**. The experimental method to form the high hardness ceramic coatings by means of the gas tunnel type plasma spraying have been described in the previous papers [5,6,7]. In this case, the gas divertor nozzle diameter was  $d=20$  mm. The power input to the pilot plasma torch (gun), which was supplied by the power supply, PS-1 was zero during spraying. The gun is a hollow cathode type, which allows the injection of powders along the centerline of the gun. All spraying experiments were conducted inside a spraying chamber, however, the chamber was not evacuated and no shroud or filler gas was used.

The experimental conditions for this plasma spraying are shown in **Table 1**. The power input to the plasma torch was about  $P=25$  kW, and the spraying distance was a short distance of  $L=40$  mm. The working gas flow rate for gas tunnel type plasma spraying torch was  $Q=180$  l/min of Ar gas, the gas flow rate of carrier gas was 10 l/min, and the powder feed rate of zirconia/alumina mixed powder was  $w=30$  g/min. The traverse speed of the substrate was changed from low value of  $v=25$  cm/min to  $v=250$  cm/min.

**Table 2** shows the chemical composition and the size of zirconia( $ZrO_2$ ) and alumina ( $Al_2O_3$ ) powder used in this study. The  $ZrO_2$  powder was commercially prepared type of K-90: 8% yttria-stabilized  $ZrO_2$ , and  $Al_2O_3$  powder was the type of K-16T. The mixing ratio of  $Al_2O_3$  to  $ZrO_2$  powder was 50- 70 wt % in this study. The substrate was SUS304 stainless steel (50x50x3t), which was sand blasted before using.

The zirconia-alumina ( $ZrO_2-Al_2O_3$ ) composite coatings produced in 30-140  $\mu m$  thickness on the substrate by plasma spraying at  $L=40$  mm, at the traverse speed of 25 cm/min, when traverse number was changed 1-4 times. On the other hand, in order to obtain the same coating thickness, the  $ZrO_2$  composite

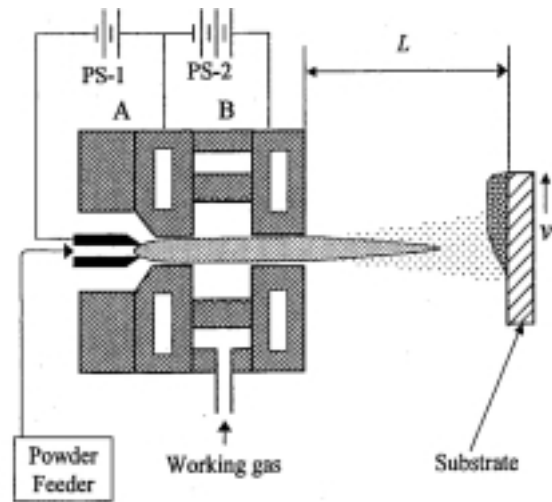


**Fig.1** Gas tunnel type plasma spraying apparatus used in this study;  $L$ : spraying distance. Gas divertor nozzle was 20 mm.

**Table 1** Experimental conditions.

Power input:	$P = 23-26$ kW
Working gas (Ar)	
flow rate:	$Q = 180$ l/min
Powder feed gas (Ar)	$Q_{feed} = 10$ l/min
Spraying distance:	$L = 40$ mm
Traverse speed:	$v = 25-1000$ cm/min
Powder feed rate:	$w = 30$ g/min

**Table 2** Chemical composition and size of zirconia powder used.

	Composition (wt%)					Size ( $\mu m$ )
	$ZrO_2$	$Y_2O_3$	$Al_2O_3$	$SiO_2$	$Fe_2O_3$	
$ZrO_2$	90.78	8.15	0.38	0.20	0.11	10-44
$Al_2O_3$	99.80	0.146	0.01	0.01		10-35

coating was formed by changing both the traverse speed and traverse number under the condition of same spraying time of 12 s.

The measurement of distribution of the Vickers hardness in the cross section of the  $ZrO_2$  coating was carried out at each distance from the coating surface in the thickness direction. The Vickers hardness of the sprayed coatings was measured at the non-pore region in those cross sections under the condition that the load weight was 50 or 100 g and its load time was 15 s. The Vickers hardness was calculated as a mean value of 10 points measurements.

The cross section of these  $ZrO_2$  composite coatings was observed with an optical microscope, at magnifications of 200 or 400. The X-ray diffraction (XRD) method was conducted on the surface of the coating. The X-ray source was Co, and the tube voltage was 30 kV and the tube current was 14 mA.

### 3. Results and Discussion

#### 3.1 Distributions of Vickers hardness on the cross section of zirconia composite coating

Figure 2 shows the distributions of Vickers hardness on the cross section of  $ZrO_2$  composite coatings produced by the gas tunnel type plasma spraying at the same traverse speed of  $v = 25$  cm/min. In this case, Ar gas flow rate was  $Q=180$  l/min, the power input:  $P=25$  kW and the spraying distance:  $L=40$  mm. And the powder feed rate was  $w=30$  g/min. These coating were formed by one time traverse, two times traverse, and 3 times traverse (3 pass sprayed). The coating thickness was approximately proportional to the traverse number, and was 60, 90, 140  $\mu\text{m}$  for 1, 2, 3 times traverse, respectively. The coating thickness per one traverse was about 50  $\mu\text{m}$  for each coating in these results.

The distribution of Vickers hardness on the cross section of  $ZrO_2$  composite coating for 1 time traverse shows one parabolic curve as shown in Fig. 2. The hardness near the coating surface was highest value of  $Hv=1140$ , much higher than that of near the coating substrate.

On the other hand, the distribution of Vickers hardness of  $ZrO_2$  composite coating for 2 times traverse consists of two parabolic curves as shown in the same figure. From this distribution, it was found that the Vickers hardness of the coating surface layer (corresponds to the second pass) was more than 1200. The highest value of this high hardness layer was about  $Hv = 1210$  at the distance from the coating surface of  $l=20-30$   $\mu\text{m}$ .

For 3 times traverse, the hardness distribution was that combined by 3 parabolic curves as shown in Fig.2. The Vickers hardness of the coating surface layer (the third pass) was highest value of about  $Hv = 1240$ . The hardness near the substrate was a lower value of  $Hv=1000$ . In this case, the hardness difference between at surface side and substrate side was much larger than the case of less time traverse. Thus, as the traverse number increased, the graded functionality of hardness became remarkable in the thickness direction.

These results were similar to the case of  $ZrO_2$  coatings obtained in the previous study. For the increase in the traverse number, the surface temperature of the coating during spraying became higher. There-

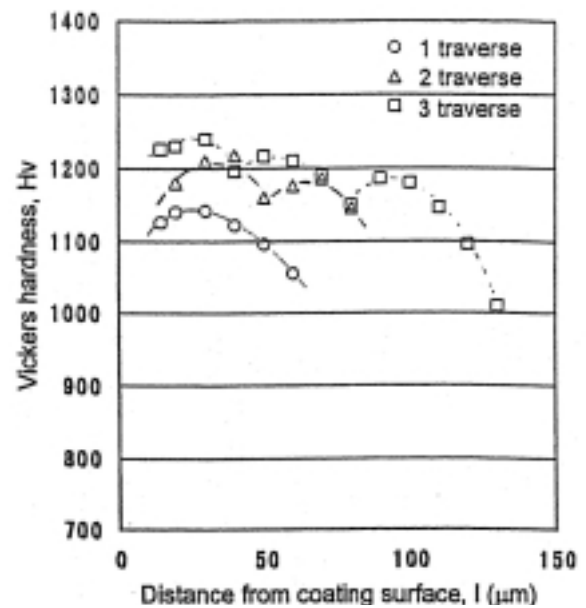


Fig.2 Distributions of Vickers hardness on cross section of zirconia composite coatings sprayed at  $L=40$ mm when  $P=25$  kW. Data plots: 1 time, 2 times and 3 times traverse.

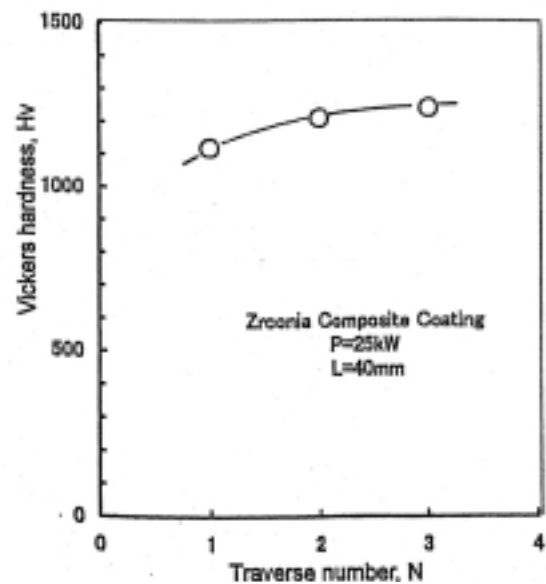


Fig.3 Dependences of Vickers hardness on the zirconia composite coatings on the traverse number at  $L=40$ mm when  $P=25$  kW.

fore it would be expected that coating density would be increased when the traverse number would be increased.

### 3.2 Dependence of Vickers hardness of zirconia composite coating on the traverse number

**Figure 3** shows the relation between the traverse number and the Vickers hardness on the surface layer of  $ZrO_2$  composite coating. In this case, those coatings for 1-3 times traverse were the same coating used in Fig. 2.

The value of Vickers hardness for each coating was increased as the traverse number was increased. The maximum hardness was increased from  $Hv = 1120$  to  $Hv = 1240$ . This would also correspond to the increase in the thickness of the coating. (60-140 $\mu m$ ) For  $ZrO_2$  coating, the dependence of Vickers hardness was the same as the  $ZrO_2$  composite coatings.

Then, in order to examine the effect of traverse number on the Vickers hardness without thickness influence, the  $ZrO_2$  composite coatings with the same thickness, was 25 cm/min for 1 time traverse, 50 cm/min for 2 times traverse, 100 cm/min for 4 times traverse and so on, under the condition:  $L=40$  mm, when  $P=25$  kW. The spraying time was about 10 seconds, and the thickness of each coating was about 140  $\mu m$  for each traverse number. In this case the mixing ratio of  $Al_2O_3$  to  $ZrO_2$  was about 70 %.

**Figure 4** shows the distributions of Vickers hardness on the cross section of  $ZrO_2-Al_2O_3$  composite coating for 1 time traverse. In Fig.4 the coating thickness was 140 $\mu m$  for 1 time traverse, and the hardness distribution was a parabolic curve. The highest value of about  $Hv = 1300$  at the distance from the coating surface of  $l=40$   $\mu m$ . This maximum hardness became much higher than that of 1 time traverse as shown in Fig.3. This would be caused by the increase in the coating thickness.

On the other hand, the  $ZrO_2$  coating of the same thickness had a little flat distribution of the Vickers hardness, whose maximum value was about  $Hv=1100$ , lower than that of the  $ZrO_2$  composite coating.

**Figure 5** shows the distributions of Vickers hardness of  $ZrO_2-Al_2O_3$  composite coating for 2-times traverse. The coating thickness was about 140 $\mu m$ , and the distribution consisted of two parabolic curves. The maximum hardness was about  $Hv = 1300$  near the coating surface of  $l=20$   $\mu m$ . The Vickers hardness of this coating was similar value in the case of three times traverse as shown in Fig.3. Also, this maximum value of  $Hv = 1300$  was almost same in those cases for 1, 4, and 10 times traverse, when the coating thickness of about 140 $\mu m$ .

It was found that the graded functionality of the Vickers hardness of this  $ZrO_2-Al_2O_3$  composite coating was much clearer than that of 1 time traverse in Fig. 4. But, the  $ZrO_2$  coating of the same thickness had a

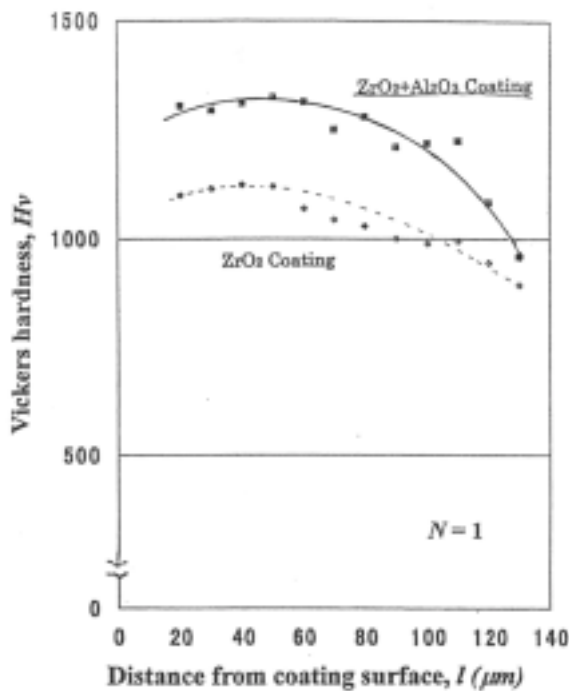


**Fig.4** Distributions of Vickers hardness on cross section of zirconia composite coatings sprayed by 1 time traverse at  $L=40$ mm when  $P=20$  kW.

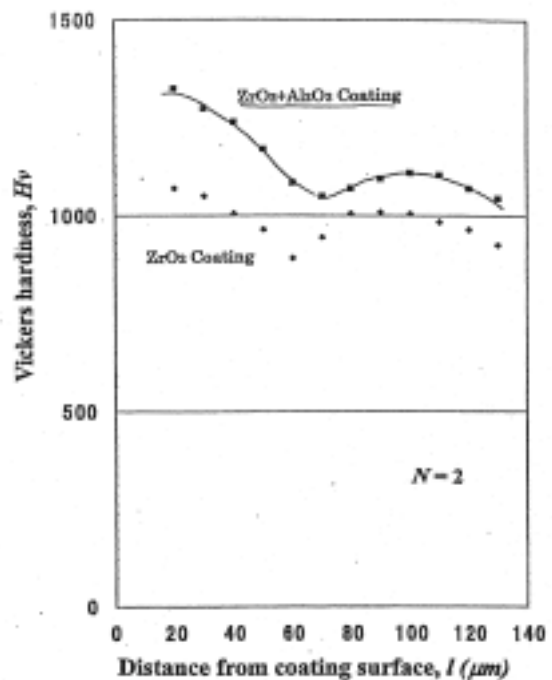


**Fig.5** Distributions of Vickers hardness on cross section of zirconia composite coatings sprayed by 2 times traverse at  $L=40$ mm when  $P=25$  kW.

more flat distribution of the Vickers hardness. The maximum value was as the same of about  $Hv=1100$  as in Fig.4.

**Figure 6** shows the hardness distribution for 30 time traverse at  $v=1000$  cm/min, when  $P=25$  kW,  $L=40$  mm. Here the coating thickness was  $150\mu\text{m}$ , and the distribution was very smooth line, without boundary of the traverse. The maximum hardness was almost near about  $Hv = 1300$  as same as Fig.5. The highest value of at the distance from the coating surface of  $l=40\mu\text{m}$ .

Thus, the maximum hardness was almost same when the coating thickness was the same. But the graded functionality became much better, and the distribution of Vickers hardness was much smoother as the traverse number was increased. The part near the substrate did not change so much, but the Vickers hardness near the coating surface became much higher than that of a few traversed coating. Therefore the graded functionality can be enhanced by the increase of the traverse number, and this leads to the development of thermally sprayed FGC.

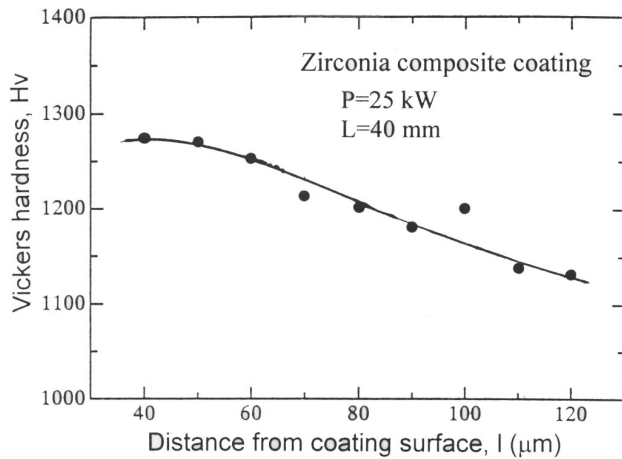


**Fig.6** Distributions of Vickers hardness on cross section of zirconia composite coatings sprayed by 30 times traverse at  $L=40\text{mm}$  when  $P=25$  kW.

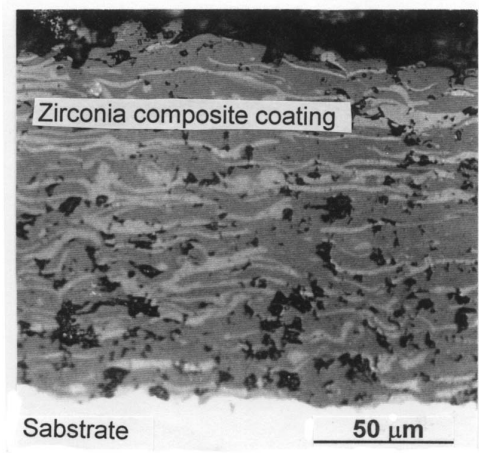


**Fig.7** Microphotograph of the cross section of  $\text{ZrO}_2$  composite coatings sprayed by 33 times traverse at  $L=40\text{mm}$  when  $P=25$  kW.

### 3.3 Structure of functionally graded zirconia composite coating

**Figure 7** shows the microphotograph of the cross section of  $\text{ZrO}_2$  composite coating. This was produced by 33 time traverse at  $P=25$  kW and  $L=40$  mm and the thickness was  $140\mu\text{m}$ . The traverse speed was about  $1000$  cm/min. In the coating, black parts were the pores and the microstructure was consisted of two areas; one is gray area, and another was white area. It was found from EPMA analysis, that the white area was  $\text{ZrO}_2$ , while gray area was  $\text{Al}_2\text{O}_3$ . Some large pores existed near the substrate, but the size and number were decreased as closing to the coating surface, and the coating density was much higher.

Thus, the microstructure of  $\text{ZrO}_2$  composite coating shows that the dense ceramic matrix composite coating with thin  $\text{ZrO}_2$  splats embedded inside a dense  $\text{Al}_2\text{O}_3$  matrix. And  $\text{ZrO}_2$  is in the form of flat stripes. This anisotropic composite coating combined with the large difference in thermal conductivity between  $\text{ZrO}_2$  and  $\text{Al}_2\text{O}_3$  will alter the thermal behavior of the coating. The coating structure might suppress the pores as compared to the  $\text{ZrO}_2$  coating as described in the previous paper.

The X-ray diffraction pattern of the surface of the composite coating is shown in **Fig.8**. This was the same coating as that in Fig. 5. There were several strong peaks

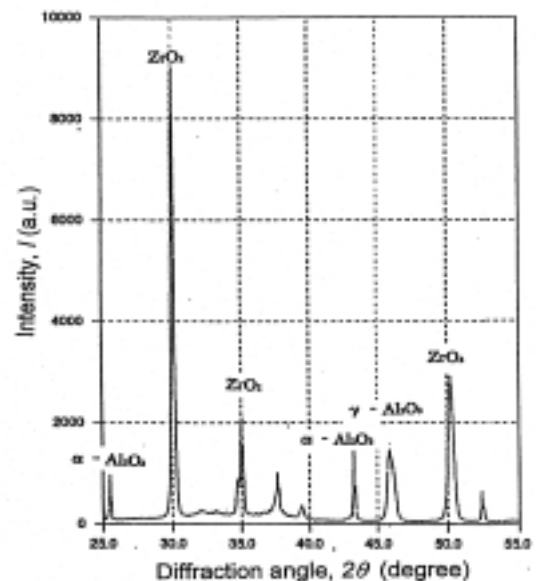


**Fig.8** X-ray diffraction patterns of zirconia composite coating for 2-times traverse in Fig.6.

of ZrO<sub>2</sub> and a few Al<sub>2</sub>O<sub>3</sub> peaks. The peak at the degree of 30 was maximum peak of ZrO<sub>2</sub>. Other peaks appeared near the degree of 35,50, and 60, respectively. The crystal form of ZrO<sub>2</sub> of powder was thought to be the cubic phase containing small amount of tetragonal ZrO<sub>2</sub> [14].

Regarding the phase of alumina in the pattern, intensity of  $\alpha$ -Al<sub>2</sub>O<sub>3</sub> peak was enough strong as shown in Fig.8. This indicates that the  $\gamma$ -Al<sub>2</sub>O<sub>3</sub> of Al<sub>2</sub>O<sub>3</sub> powder was transformed to  $\alpha$ -Al<sub>2</sub>O<sub>3</sub> by high energy plasma spraying process.

#### 4. Conclusion

The functionally graded thermal barrier ZrO<sub>2</sub>-Al<sub>2</sub>O<sub>3</sub> composite coatings were formed by the gas tunnel type plasma spraying, and the coating properties were investigated, and the following results were obtained.

- (1) The distribution of Vickers hardness on the cross section of those coatings consists of the traverse number of parabolic curves in the thickness direction for 1-3 times traverse spraying. And higher value of Vickers hardness was obtained as compared pure ZrO<sub>2</sub> coating.
- (2) With increase in the traverse number, Vickers hardness of the high hardness layer became higher value, which was changed from  $Hv=1120$  to  $Hv=1240$ , under the spraying condition:  $P=25$  kW,  $L=40$  mm. It was caused by the increase in the coating thickness. Because, the coating thickness was changed from 60 to 140  $\mu$ m,
- (3) The graded functionality was enhanced by the increase in the traverse number. Also, the hardness distribution became smoother as the number. Enhancement of graded functionality should be achieved by controlling the traverse number and the coating thickness.
- (4) The microstructure of ZrO<sub>2</sub> composite coating showed that the dense ceramic matrix composite coating with ZrO<sub>2</sub> splats embedded inside a dense Al<sub>2</sub>O<sub>3</sub> matrix. The crystal form of the cubic ZrO<sub>2</sub> and tetragonal phase,  $\alpha$ -Al<sub>2</sub>O<sub>3</sub>, and  $\gamma$ -Al<sub>2</sub>O<sub>3</sub> composed this composite coating.

#### Acknowledgements

This study was financially supported in part by a Grant-in-Aid for Scientific Research from the Japanese Ministry of Education, Science and Culture, and The Iwatani Naoji Foundation.

#### References

- [1] S. Sampath, R. Gansert, H. Herman, JOM **47**-10 (1995), p30-33.
- [2] Composites and functionally graded materials; *Proceedings of the Symposia, 1997 ASME International Mechanical Engineering Congress and Exposition*, Dallas, TX, Nov. (1997), p16-21
- [3] Y. Arata, A. Kobayashi, Y. Habara, S. Jing. *Trans. of JWRI*, **15** (1986), p227-231.
- [4] Y. Arata, A. Kobayashi, and Y. Habara: *J. Applied Physics*, **62**(1987) pp.4884-4889
- [5] Y. Arata, A. Kobayashi, and Y. Habara, *J. High Temp. Soc.*, **13** (1987), p116-124.
- [6] A. Kobayashi, S. Kurihara and Y. Arata, *J. High Temp. Soc.*, **15** (1989), p210-216.
- [7] A. Kobayashi, S. Kurihara, Y. Habara, Y. Arata; *J. Weld. Soc. Jpn.*, **8** (1990), p457-463.
- [8] A. Kobayashi. *Proc. of ITSC.*, (1992), p57-62.
- [9] A. Kobayashi: *J. of Thermal Spray Technology*, **Vol.5** (1996) pp.298-302.
- [10] A. Kobayashi. *Surface and Coating Technology*, Vol.**90**, (1997), p197-202
- [11] A. Kobayashi, T. Kitamura. *J. of IAPS Applied Plasma Science*, **5**(1997), p62-68.
- [12] A. Kobayashi, T. Kitamura: *Advances in Applied Plasma Science*, **Vol.2** (1999) pp.223-229,
- [13] A. Kobayashi, T. Kitamura. *J. High Temp. Soc.*, **26** (2000), p316-320.
- [14] R.A. Miller, J.L. Smialek, R.G. Garlick. *Am. Ceram. Soc.*, **3** (1981), p241.

# IEPC 2003

2003. 1.14

*\*Corresponding Author:*

**Akira Kobayashi**  
JWRI, Osaka University  
11-1 Mihogaoka,  
Ibaraki, Osaka 567-0047, Japan  
Fax: 06-6879-8689  
Email: [kobayasi@jwri.osaka-u.ac.jp](mailto:kobayasi@jwri.osaka-u.ac.jp)